Optical Spin Hall Effects in Plasmonic Chains

ARTICLE *in* NANO LETTERS · MAY 2011

Impact Factor: 13.59 · DOI: 10.1021/nl2004835 · Source: PubMed

NANO LETTERS

LETTER

pubs.acs.org/NanoLett

Optical Spin Hall Effects in Plasmonic Chains

Nir Shitrit, Itay Bretner, Yuri Gorodetski, Vladimir Kleiner, and Erez Hasman*

Micro and Nanooptics Laboratory, Faculty of Mechanical Engineering, and Russell Berrie Nanotechnology Institute, Technion—Israel Institute of Technology, Haifa 32000, Israel

ABSTRACT: Observation of optical spin Hall effects (OSHEs) manifested by a spin-dependent momentum redirection is presented. The effect occurring solely as a result of the curvature of the coupled localized plasmonic chain is regarded as the *locally isotropic* OSHE, while the *locally anisotropic* OSHE arises from the interaction between the optical spin and the local anisotropy of the plasmonic mode rotating along the chain. A wavefront phase dislocation was observed in a circular curvature, in which the dislocation strength was enhanced by the *locally anisotropic* effect.

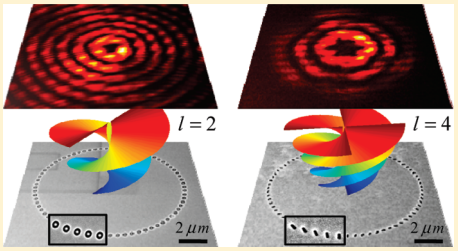

KEYWORDS: Plasmonics, optical spin Hall effect, angular momentum, polarization

The spin Hall effect is a basic phenomenon arising from the spin−orbit coupling of electrons.[1] In particular, the spatial trajectory of the moving electrons is affected by their intrinsic angular momentum. More generally, the dispersion relation of the particles is modified in a spin-dependent manner.[2] The spin Hall effect is regarded as intrinsic when it arises due to Rashba coupling (Berry curvature),[3] while the extrinsic effect occurs due to the spin−orbit-dependent scattering of electrons from impurities.[4] The optical spin Hall effect (OSHE)—beam displacement and momentum shift due to the optical spin (polarization helicity)—was recently presented.[5−9] The effect was attributed to the optical spin−orbit interaction occurring when the light passes through an anisotropic and inhomogeneous medium. Here, we present and experimentally observe the optical spin Hall effects in coupled localized plasmonic chains. The *locally isotropic* optical spin Hall effect (OSHE-LI) is regarded as the interaction between the optical spin and the path ξ of the plasmonic chain with an isotropic unit cell (Figure 1a). In contrast, the *locally anisotropic* optical spin Hall effect (OSHE-LA) occurs due to the interaction between the optical spin and the local anisotropy of the unit cell, which is independent of the chain path (Figure 1b). This latter mechanism expands the scope of the OSHE and provides an additional degree of freedom in spin-based optics.

Localized surface plasmons are nonpropagating excitations of the conduction electrons of metallic nanostructures coupled to the electromagnetic field. The localized plasmonic modes were found to play a key role in extraordinary light concentration by metallic nanofeatures.[10] A localized field can be formed by a nanoscale structure characterized by an omnidirectional reemission. By introducing a coupled nanostructure chain, the individual localized mode can be tailored to a collective mode—coupled localized mode of the whole chain, having a directional reemission.[11−13] Due to a low dimensionality of the chain, the excitation of the plasmonic chain mode is polarization-dependent, which leads to anisotropic scattering.

A coupled plasmonic chain was fabricated by focused ion beam (FIB; FEI Strata 400s dual beam system, Ga^+, 30 keV, 46 pA) etching upon a thin (200 nm) Au film, deposited on a glass substrate (Figure 2a, inset). The chain consisted of isotropic unit cells—coaxial nanoapertures with radii of 75 and 125 nm—arranged in a single line with a period Λ of 470 nm. The fabricated element was immersed in an index-matching oil to obtain symmetric configuration. The coaxial shape of the aperture was chosen due to its well-proven ability of plasmon localization.[14] The transmission spectrum of the coupled plasmonic chain was found to bear a signature of two modes centered at the wavelengths of 700 and 780 nm corresponding to transversal and longitudinal polarization excitations,[15] respectively (Figure 2a).

In order to study the OSHE-LI, we fabricated a chain whose local orientation with respect to the x coordinate $\theta = \tan^{-1}(dy/dx)$ varies linearly with x, explicitly, $\theta(x) = \pi x/a$ where a is the rotation period of the structure (Figure 2b). This demand leads to a chain with a route $\{x(\xi),y(\xi)\}$ given by the function $\xi = (a/2\pi)\ \ln[(1 + \sin(\pi x/a))/(1 - \sin(\pi x/a))]$. The local orientation of the curved chain induces local anisotropy variation in the scattered field. The experimental setup to study the OSHEs is introduced in Figure 2c. Figure 2d shows the measured OSHE-LI observed from the chain. The structure was sandwiched between circular polarizers and illuminated with a continuous wave Ti:sapphire tunable laser (Spectra-Physics 3900S) at a wavelength of 780 nm in order to excite the longitudinal mode. The intensity distribution was measured in the far-field, which corresponds to the momentum space. Polarization analysis shows that the scattering from the curved chain comprises two components: ballistic and spin-flip. The ballistic component does not experience any diffraction and maintains the polarization state of the incident beam, while the spin-flip component, with an opposite spin state, undergoes diffraction. Spin-dependent beam deflection is observed in the experiment via orthogonal circular polarizers and corresponds to a momentum shift of $\Delta k_x = -2\sigma\pi/a$, where $\sigma = \pm 1$ is the incident spin state.

Received: February 10, 2011
Revised: April 11, 2011
Published: April 22, 2011

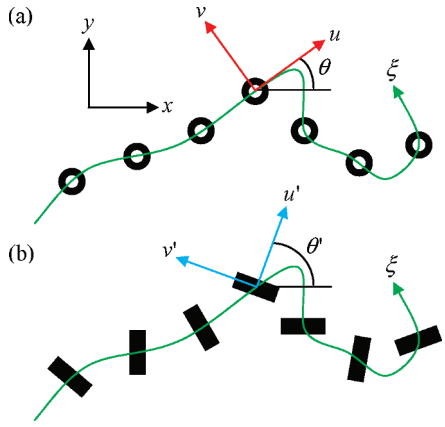

Figure 1. Coupled localized plasmonic chains. (a) A plasmonic chain with isotropic unit cell and rotating reference frame (u,v) which follows the path ξ. (b) An anisotropy unit cell chain with a frame (u',v') attached to the local anisotropy axis of the unit cell. The lab reference frame is indicated by (x,y).

The peculiarity of the observed effect lies in its geometric nature. Light scattering by a system with spatially nonuniform anisotropy has a close analogy with a scattering from a revolving medium,[16] as was shown recently.[17] Hence, the scattering by the bent chain is most conveniently studied using a rotating reference frame[17,18] (u,v), which is attached to the axis of the local anisotropy of the chain and follows the chain's route $\xi(x,y)$ (Figure 1a). This is accompanied by spatial rotation of the frame with a rate $\Omega_\xi = d\theta(\xi)/d\xi$, where $\theta(\xi)$ is the orientation angle. As a result, a spin-dependent momentum deviation $\Delta k_\xi = -2\sigma\Omega_\xi$ which corresponds to an additional phase of $\phi = \int \Delta k_\xi d\xi = -2\sigma\theta$, appears in the spin-flip scattered component. The experimentally observed spin Hall momentum deviation concurs with the expected correction of $\Delta k_x = \nabla_x\phi = -2\sigma\pi/a$. This effect is regarded as the OSHE-LI.

When the chain unit cell is anisotropic itself, the local anisotropy is also allowed to be arbitrarily oriented along the path. The reference frame attached to the unit cell anisotropy is presented as the system (u',v') in Figure 1b. It was previously shown that plasmonic structures consisting of nanorods exhibit a high polarization anisotropy that follows the orientation of the rods.[19,20] An element consisting of randomly arranged but similarly oriented rectangular apertures with dimensions of 80 × 220 nm was fabricated (Figure 3a, top inset). The localized mode resonance of this array was obtained at a wavelength of 730 nm by measuring the transmission spectrum with linear polarization excitation parallel to its minor axis. High anisotropy is clearly observed between the two orthogonal linear polarization excitations, which results from the local anisotropy of the nanorod (Figure 3a). Next, we fabricated a straight chain of subwavelength nanorods with a period of 430 nm (Figure 3a, bottom inset) in correspondence with the momentum matching condition and obtained a narrow resonant line shape of the transmitted light, when the structure was excited by a linear polarization parallel to the nanorod's minor axis (Figure 3a). The orientation of the nanorods was then varied linearly along the x axis to obtain a spatial rotation rate of $\Omega = d\theta'/dx = \pi/a$ (Figure 3b). The far-field intensity scattered from the element was analyzed using the same setup as before and the beam deflection of the spin-flip component corresponding to the spin Hall momentum deviation of $\Delta k_x = -2\sigma\Omega$ was detected

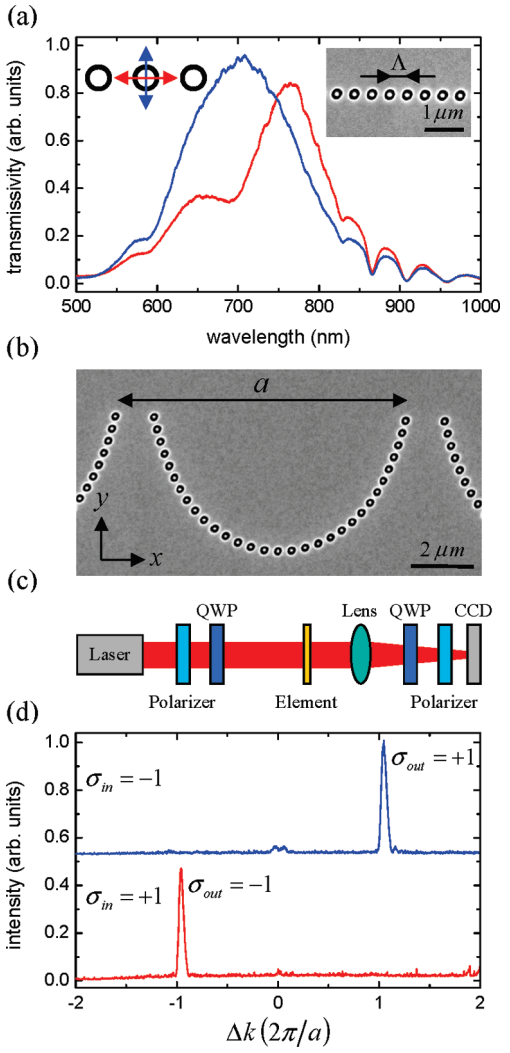

Figure 2. (a) Transmission spectra of the plasmonic chain consisting of coaxial nanoapertures with inner/outer radii of 75/125 nm, with period of Λ = 470 nm and a length of 84.6 μm. The blue and red lines/arrows correspond to transversal and longitudinal polarization excitations, respectively. The inset shows a scanning electron microscopy (SEM) image of the chain. (b) SEM image of a curved chain whose local orientation θ is varied linearly along the x axis with a rotation period of a = 9 μm, and a structure length of 135 μm. (c) Experimental setup for OSHE measurement. A laser light beam passes through a circular polarizer (a linear polarizer followed by a quarterwave plate (QWP)) and then is incident onto the element. The emerging light is collected by an imaging lens to a CCD camera after polarization analysis with a circular polarizer−analyzer. (d) The spin-dependent momentum deviation for the OSHE-LI, at a wavelength of 780 nm. The red and blue lines stand for incident right- and left-handed circularly polarized light, respectively ($\sigma_{in} = \pm 1$). σ_{out} denotes the spin state of the scattered light.

(Figure 3c). This beam deflection is regarded as the OSHE-LA and it arises due to the rotation of the local unit cell's anisotropy rather than the chain path curvature.

Our described mechanism paves the way for one to consider other path symmetries. According to Noether's theorem,[21] for every symmetry there is a corresponding dynamical conservation law.[22] When the structure symmetry, or more explicitly the chain path $\xi(x,y)$, is circular, the corresponding conservation rule is for the angular momentum (AM). The AM of an optical beam can

dx.doi.org/10.1021/nl2004835 |Nano Lett. 2011, 11, 2038–2042

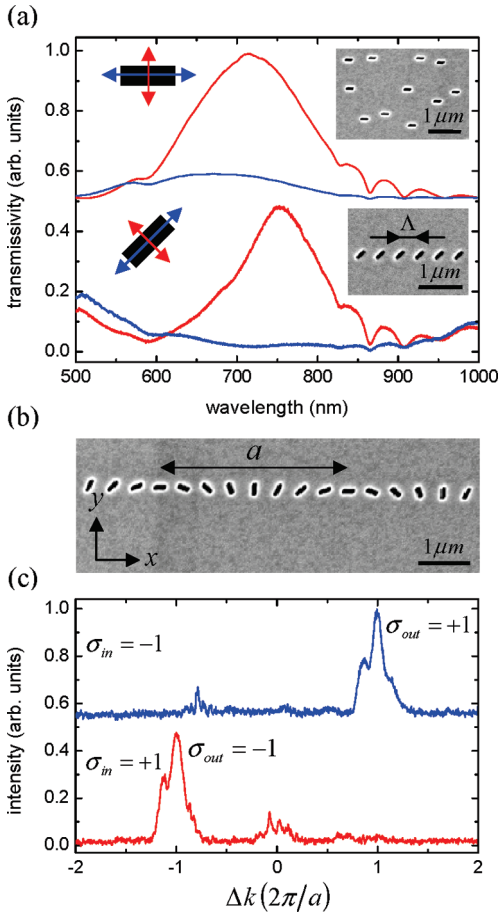

Figure 3. (a) Transmission spectra of randomly arranged identically oriented rectangular apertures with dimensions of 80 × 220 nm in 86 μm square array, and of a homogeneous chain with period Λ = 430 nm, local orientation $\theta' = 45°$ and a length of 86 μm. The red and blue lines/arrows correspond to linear polarization excitations parallel and perpendicular to the nanorod's minor axis, respectively. The insets show SEM images of the structures described above. (b) SEM image of a chain in which the nanorods' orientation θ' varies linearly along the x axis with a rotation period of a = 3.44 μm, and a structure length of 86 μm. (c) The spin-dependent momentum deviation for the OSHE-LA, at a wavelength of 730 nm. The red and blue lines stand for incident spin states $\sigma_{in} = \pm 1$, respectively.

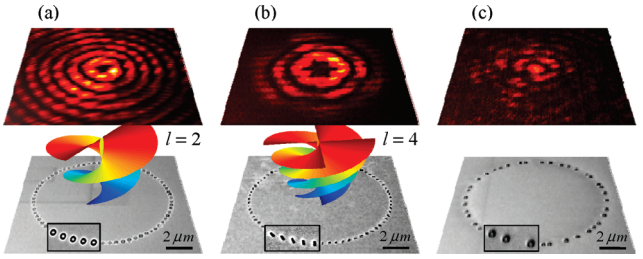

Figure 4. The OSHE-LI and OSHE-LA for circular chains. The measured far-field intensity distribution of the spin-flip component scattered from a circular chain of ordered (a) and disordered (c) coaxial apertures at a wavelength of 780 nm and rotating nanorods with $m = 2$ at a wavelength of 730 nm (b). Bottom, SEM images of the chains with radii of r_o = 5 μm. The spin Hall momentum deviation is accompanied by a spiral phase-front with $l = 2$ and $l = 4$, for the OSHE-LI (a) and OSHE-LA (b), respectively. Note that no spin Hall momentum deviation is observed from the disordered chain (c).

have two components: an intrinsic component that is associated with the handedness of the optical spin, and an extrinsic (orbital) component that is associated with its spatial structure. In an optical paraxial beam with a spiral phase distribution ($\phi = -l\varphi$, where φ is the azimuthal angle in polar coordinates and the integer number l is the topological charge), the total AM per photon, in units of $\hbar$ (normalized AM), was shown to be $j = \sigma + l$.[23] We fabricated circular chains with a path parameter $\xi = r_o\varphi$ (r_o is the chain radius) of coaxial apertures and rotating nanorods with a rotation rate $\Omega = m/r_o$, so the local anisotropy orientation is $\theta' = m\varphi$ (m is an integer). The far-field intensity distributions of the scattered spin-flip components were measured using the experimental configuration described earlier (see panels a and b of Figure 4 for coaxial apertures and rotating nanorods with m = 2, respectively). A characteristic dark spot in the center is clearly seen in the images which is a signature of orbital AM. Moreover, it is evident that the radius of the dark spot measured with the nanorod chain of $m = 2$ is larger than the one measured with the coaxial apertures, corresponding to a higher orbital AM. The observed OSHEs and specifically the orbital AM obtained from circular chains are due to the collective interaction of the localized modes within the periodic plasmonic chains. To verify the role of the interaction, we measured the spin-flip component of the scattered light from a circular chain with random distribution of coaxial apertures. As evident from Figure 4c, a bright spot was obtained, indicating zero orbital AM in a disordered plasmonic chain.

The orbital AM of the spin-flip component scattered from a circular chain is characterized by the strength of the dislocation and its helicity. Phase dislocations are singular field points such that the phase obtains a 2π-fold jump when making a closed loop around them. The dislocation's strength is the number of wave fronts that end at the phase dislocation point. Its absolute value and sign (helicity) can be measured simultaneously by the interference of two optical vortices.[24,25] For this purpose, an element consisting of two separated identical chains of nanorods rotated along a circular path with $m = 1$ was fabricated (Figure 5a, b). The two chains, which behave as twin sources, give rise to intensity fringes, as shown in panels f and g of Figure 5. In the measured interference patterns of the spin-flip components, two additional fringes emerge, indicating two phase dislocations (see the guiding lines in panels f and g of Figure 5). When we alter the incident spin state, the antisymmetric forklike picture is reversed. The experimental patterns with an incident spin of $\sigma = \pm 1$ are similar to calculated patterns resulting from the scalar interference of two identical optical vortices with topological charges of $l = \pm 2$, respectively (Figure 5d,e). The spin-dependent fringe patterns of a similar element with $m = -1$ (Figure 5c) were also measured (not shown) to verify that the helicity of the phase dislocation corresponds to the rotation handedness of the nanorods. Moreover, the interference pattern of the ballistic component did not comprise a phase dislocation, indicating zero orbital AM. Each of the phase dislocations of the spin-flip components predicted by the calculated patterns (triple fork, see panels d and e of Figure 5), breaks in the experiment into a pair of fundamental phase dislocations (double fork, see panels f and g of Figure 5). The nongeneric vortex collapse to generic vortices is in accordance with the prediction in ref 26; therefore, the topological charge of the beam in this experiment is given by the number of the fundamental phase dislocations, resulting in

dx.doi.org/10.1021/nl2004835 |Nano Lett. 2011, 11, 2038–2042

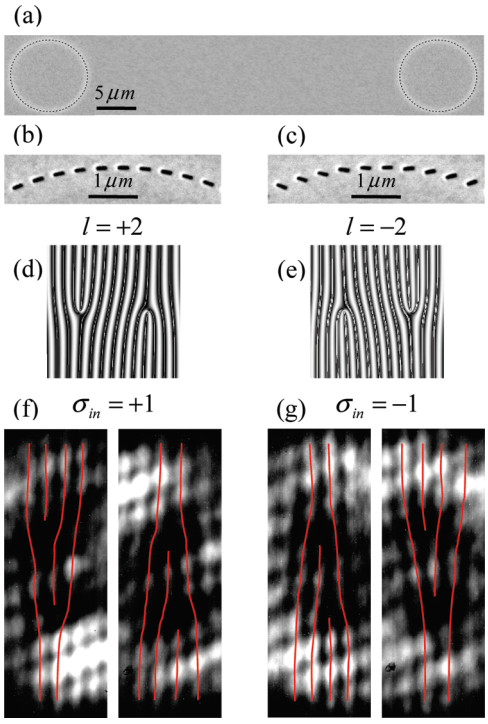

Figure 5. Dislocation's strength measurement. (a) SEM image of two separated identical chains of nanorods rotated along a circular path with $m = 1$. (b, c) Magnified segments of SEM images of circular chains with $m = \pm 1$, respectively. (d, e) Calculated interference patterns for a pair of identical optical vortices with topological charges of $l = \pm 2$, respectively. (f, g) Measured interference patterns of the spin-flip components for $m = 1$ (regions of interest), at a wavelength of 730 nm and incident spin states $\sigma_{in} = \pm 1$, respectively. The additional fringes emerge above or below indicate the two generic phase dislocations and the red guiding lines emphasize their locations.

$l = \pm 2$. As the orbital AM is directly linked to the azymuthal momentum correction Δk_φ via $l = -(1/2\pi)\oint \Delta k_\varphi \, d\xi$, the observed optical field with $l = 2m\sigma$ provides the evidence for a spin Hall momentum deviation of $\Delta k_\varphi = -2m\sigma/r_o$. Since the unit cell anisotropy of the chain for $m = 1$ follows its curvature ($\theta' = \varphi$), the OSHE-LA in this case is equivalent to the OSHE-LI one. However, by m-fold rotation of the nanorods' orientation one can obtain m-fold magnification of the OSHE. Circular chains of coaxial apertures and rotating nanorods with $m = \pm 2$ were analyzed using the same interference method to experimentally demonstrate that the topological charge of the spin-flip component equals $l = 2\sigma$ and $2m\sigma$ for the OSHE-LI and OSHE-LA, respectively.

In addition, we verified the topological charge's magnitude of the spin-flip component scattered from the circular chains by an interference results from a linear polarization projection of the ballistic and the spin-flip components. We measured the intensity distribution immediately behind the element via a linear polarizer. The interference patterns obtained by circular chains of coaxial apertures and rotating nanorods with $m = 1,2$ are visualized in Figure 6. Propeller-like images confirm the orbital AM of l, which is expected from the obtained interference profile of $1 + \cos(l\varphi)$, for the OSHE-LI and OSHE-LA.

In summary, we observed the optical spin Hall effect in plasmonic coupled localized mode chains. The OSHEs in our plasmonic chains are geometric in nature and observed in achiral

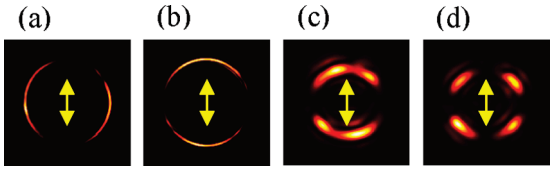

Figure 6. Interference patterns resulting from linear polarization projections of the ballistic and spin-flip components scattered from single circular chains of coaxial apertures (a, b), rotating nanorods with $m = 1$ (c) and $m = 2$ (d). The arrows indicate the direction of the linear polarizer−analyzer. The coaxial chain was illuminated at wavelengths of 780 and 700 nm to excite the longitudinal (a) and transversal (b) plasmonic modes, respectively. The nanorod chain was illuminated at 730 nm.

structures consisting of achiral nanoscatterers. The effect occurring solely due to the curvature of the chain was regarded as the OSHE-LI, in contrast with the OSHE-LA arising as a result of the unit cell's local anisotropy rotation along the chain. The intrinsic AM of the incident light is coupled to the extrinsic linear or orbital momentum of the emerging beam via the spin−orbit interaction. Compared to the OSHE-LI in circular symmetry, the OSHE-LA provides an additional degree of freedom for optical AM generation, which may be utilized for nanoparticle rotation and tweezing by plasmonic vortices.[27] We believe that the presented concepts may lead to novel spinoptical devices as well as serve as the basis for a fundamental research in nanophotonics.

AUTHOR INFORMATION

Corresponding Author

*E-mail: mehasman@tx.technion.ac.il.

REFERENCES

(1) Dyakonov, M. I.; Perel, V. I. *Phys. Lett. A* **1971**, *35*, 459.
(2) Bychkov, Y. A.; Rashba, E. I. *J. Phys. C* **1984**, *17*, 6039.
(3) Sinova, J.; Culcer, D.; Niu, Q.; Sinitsyn, N. A.; Jungwirth, T.; MacDonald, A. H. *Phys. Rev. Lett.* **2004**, *92*, 126603.
(4) Gradhand, M.; Fedorov, D. V.; Zahn, P.; Mertig, I. *Phys. Rev. Lett.* **2010**, *104*, 186403.
(5) Leyder, C.; Romanelli, M.; Karr, J. Ph.; Giacobino, E.; Liew, T. C. H.; Glazov, M. M.; Kavokin, A. V.; Malpuech, G.; Bramati, A. *Nat. Phys.* **2007**, *3*, 628.
(6) Hosten, O.; Kwait, P. *Science* **2008**, *319*, 787.
(7) Bliokh, K. Y.; Niv, A.; Kleiner, V.; Hasman, E. *Nat. Photonics* **2008**, *2*, 748.
(8) Bliokh, K. Y.; Shadrivov, I. V.; Kivshar, Y. S. *Opt. Lett.* **2009**, *34*, 389.
(9) Aiello, A.; Merano, M.; Woerdman, J. P. *Phys. Rev. A* **2009**, *80*, 061801.
(10) Li, K.; Stockman, M. I.; Bergman, D. J. *Phys. Rev. Lett.* **2003**, *91*, 227402.
(11) Ebbesen, T. W.; Lezec, H. J.; Ghaemi, H. F.; Thio, T.; Wolff, P. A. *Nature* **1998**, *391*, 667.
(12) Alaverdyan, Y.; Sepúlveda, B.; Eurenius, L.; Olsson, E.; Käll, M. *Nat. Phys.* **2007**, *3*, 884.
(13) Curto, A. G.; Volpe, G.; Taminiau, T. H.; Kreuzer, M. P.; Quidant, R.; van Hulst, N. F. *Science* **2010**, *329*, 930.
(14) Fan, W.; Zhang, S.; Minhas, B.; Malloy, K. J.; Brueck, S. R. J. *Phys. Rev. Lett.* **2005**, *94*, 033902.
(15) Maier, S. A.; Brongersma, M. L.; Kik, P. G.; Atwater, H. A. *Phys. Rev. B* **2002**, *65*, 193408.
(16) Garetz, B. A. *J. Opt. Soc. Am.* **1981**, *71*, 609.

(17) Bliokh, K. Y.; Gorodetski, Y.; Kleiner, V.; Hasman, E. *Phys. Rev. Lett.* **2008**, *101*, 030404.
(18) Lipson, S. G. *Opt. Lett.* **1990**, *15*, 154.
(19) Gordon, R.; Brolo, A. G.; McKinnon, A.; Rajora, A.; Leathem, B.; Kavanagh, K. L. *Phys. Rev. Lett.* **2004**, *92*, 037401.
(20) Koerkamp, K. J. K.; Enoch, S.; Segerink, F. B.; van Hulst, N. F.; Kuipers, L. *Phys. Rev. Lett.* **2004**, *92*, 183901.
(21) Noether, E. *Nachr. K. Ges. Wiss. Göttingen, Math-Phys. Kl.* **1918**, 235.
(22) Koralek, J. D.; Weber, C. P.; Orenstein, J.; Bernevig, B. A.; Zhang, S.-C.; Mack, S.; Awschalom, D. D. *Nature* **2009**, *458*, 610.
(23) Allen, L.; Beijersbergen, M. W.; Spreeuw, R. J. C.; Woerdman, J. P. *Phys. Rev. A* **1992**, *45*, 8185.
(24) Sztul, H. I.; Alfano, R. R. *Opt. Lett.* **2006**, *31*, 999.
(25) Brasselet, E.; Murazawa, N.; Misawa, H.; Juodkazis, S. *Phys. Rev. Lett.* **2009**, *103*, 103903.
(26) Soskin, M. S.; Gorshkov, V. N.; Vasnetsov, M. V.; Malos, J. T.; Heckenberg, N. R. *Phys. Rev. A* **1997**, *56*, 4064.
(27) Liu, M.; Zentgraf, T.; Liu, Y.; Bartal, G.; Zhang, X. *Nat. Nanotechnol.* **2010**, *5*, 570.